

Wettability of AlN with different roughness, porosity and oxidation state by commercial Ag-Cu-Ti brazes

N. YU. TARANETS*, H. JONES

Department of Engineering Materials, The University of Sheffield, Sir Robert Hadfield Building, Mappin Str., Sheffield, S1 3JD, UK
E-mail: n.taranets@sheffield.ac.uk

The effects of porosity (about 27%), of roughness ($R_a = 0.17\text{--}0.20\ \mu\text{m}$ versus $R_a = 0.02\text{--}0.03\ \mu\text{m}$) and of pre-oxidation (air, 1250°C , 30 min) on wettability and contact interaction of AlN with commercial brazing alloys of Ag-Cu-Ti composition were studied. Wettability was determined by the sessile drop method. The interface interaction was identified by SEM and microprobe analysis. Experimental data for porous, pre-oxidized and rough samples are compared with data for dense samples polished to $R_a = 0.02\text{--}0.03\ \mu\text{m}$ not subjected to pre-oxidation. The results show that for these systems surface roughness does not influence the contact angle value significantly. Pre-oxidation of the AlN, however, tends to reduce wettability as a result of the replacement of braze/AlN interaction by braze/surface aluminium oxide interaction. Contact angles for porous samples are higher by about $20\text{--}30^\circ$ than for dense samples. © 2005 Springer Science + Business Media, Inc.

1. Introduction

Oxidation, porosity and roughness are typical surface conditions that apply to non-oxide ceramics involved in industrial manufacturing processes. The influence of these conditions on the contact angle and interaction for high temperature wetting alloy/solid systems, such as ceramic/Ti-containing alloy systems, has not been studied very much experimentally.

Compared with non-oxidized TiC, pre-oxidation enhanced wetting of TiC by Me-Al (Me: Au, Ag, Cu, Sn) alloys [1]. According to [2], contact angles of Sn and Ni on oxidized α -SiC are governed up to 1600 K by the presence of a SiO₂ film on the surface. The actual interface SiC/Me is developed only when fragmentation of the SiO₂ takes place at temperatures above 1600 K. The SiC/Me interface thus develops in course of time during such isothermal exposure, as for the system oxidized SiC/Cu-Si [3]. Only one work is known to the authors which reports on contact angles of Ag-Cu-Ti alloys in contact with a pre-oxidized ceramic: pre-oxidation of SiC leads to an increase in contact angles [4].

Previous experimental results indicate that porosity in AlN tends to decrease its wettability by liquid alloys for both wetting (AlN/Sn-Al [5]) and non-wetting (AlN/Cu [6]) cases. This holds true as well for the ZrO₂/Mn system [7].

A study [8], performed for the systems quartz/Cu, Sn and Sn-Ti indicated a rise in contact angle with increasing roughness for both wetting and non-wetting.

Investigation [9] showed that the TiN/Al system is not as sensitive to roughness as the TiN/AlSi11 system, because of formation of a rough interfacial layer between TiN and Al. According to ref. [10] an increase in roughness is accompanied by an insignificantly higher value of contact angle and a significantly longer time to reach its final value for the Al/AlN system.

The present purpose is to explore the effect of pre-oxidation, porosity and roughness on the contact angle and interface interactions between AlN and two commercially available active Ag-Cu-Ti brazing alloys (CB4 and CB5).

2. Experimental procedure

The sessile drop method was used for the contact angle measurements. The vacuum furnace employed has been described elsewhere [4]. Fully dense AlN, made by liquid phase sintering with up to 3–5 wt% YAlO₃ as a sintering aid, was supplied by the Saint Gobain Company. Porous samples (porosity $\sim 27\%$, pore diameter 1–6 μm) was obtained by sintering in nitrogen without sintering aids. Two brazing alloys, CB4(70.5Ag-26.5Cu-3Ti: wt%) and CB5(64Ag-34.2Cu-1.8Ti: wt%) were supplied by the BrazeTec GmbH as wire 3 mm in diameter which was cut into cylinders of height about 3 mm and mass about 0.2 g.

Experiments were performed under a vacuum better than 1×10^{-3} Pa. Temperature was raised at 3 K/min up

* Author to whom all correspondence should be addressed.

to 810°C and at 4 K/min above 810°C. The time when the furnace reached 810, 900 or 950°C was designated as zero time for contact angle measurements. Contact angle and the base diameter of the drop were measured as a function of time.

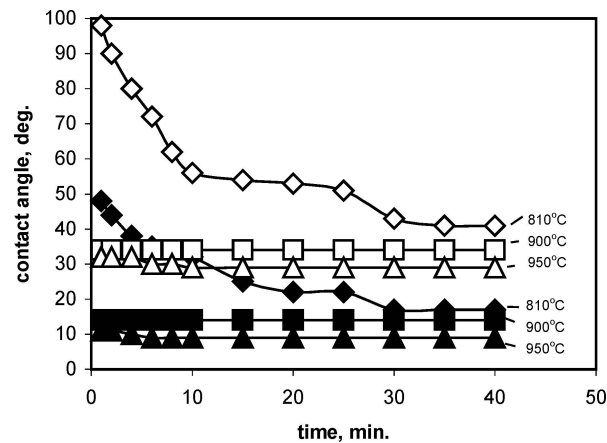
Dense substrates for experiments were fully polished to Ra = 0.02–0.03 μm or partially polished to Ra = 0.17–0.20 μm. Pre-oxidation was performed in air at 1250°C for 30 min on fully polished samples. Porous samples were also fully polished.

Some samples were subsequently cross-sectioned and prepared for SEM. A JEOL JXA-880R microprobe was used for the dense samples and a JEOL 6400 SEM equipped with EDS for the porous samples.

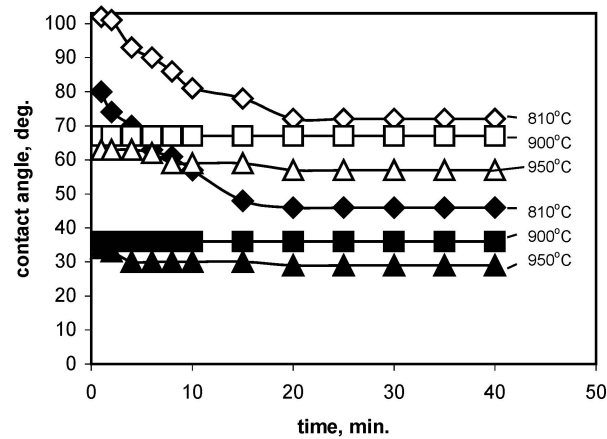
3. Results

Fig. 1a and b show the effect of porosity on contact angle θ versus time curves at different temperatures. Contact melting and spreading was observed while drops were in their melting range 780–810°C. Both alloys wet dense AlN effectively, but CB4, with higher Ti content, wets AlN better.

The porous AlN is wetted less effectively, θ being higher by about 20–30°, although the form of time dependencies and the time to reach the final θ are very similar to those for dense AlN.

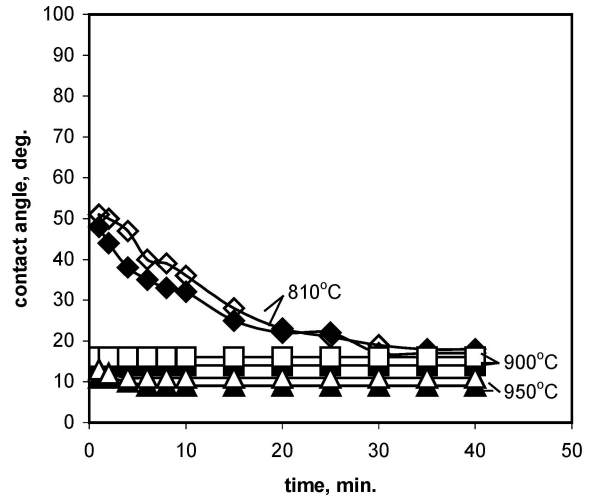


(a)

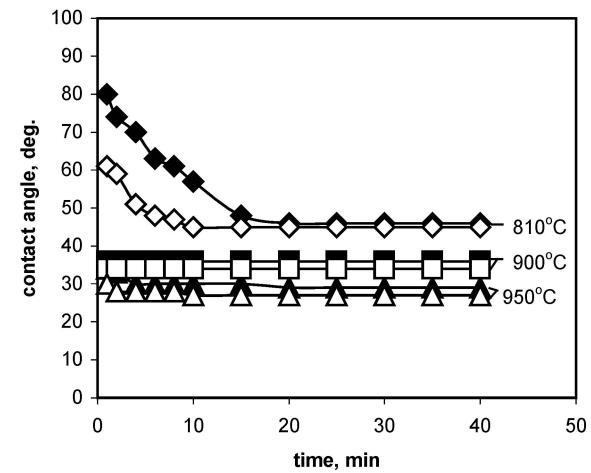


(b)

Figure 1 Time and temperature dependencies for the contact angles of CB4 (a) and CB5 (b) melts on fully polished dense AlN (closed points) and porous AlN (open points).



(a)



(b)

Figure 2 Time and temperature dependencies of contact angles for (a) CB4 and (b) CB5 melts on AlN of roughness Ra = 0.17–0.20 μm (open points) in comparison with fully polished samples (Ra = 0.02–0.04 μm) (closed points).

Fig. 2a and b show that the systems under study are not very sensitive to change of roughness levels with the final θ values and the times to reach them being very similar for the two levels of roughness.

Time-temperature dependencies of contact angle (Fig. 3a and b) for surfaces with and without pre-oxidation show as a whole worse wettability after pre-oxidation. However, the presence of the oxide film does not influence the time of spreading.

The interaction layers for CB4 and CB5 melts have similar microstructures (Fig. 4a and b). The interaction zone consists of a narrower layer 1 succeeded on the metal side by a slightly wider layer 2, the latter containing visible inclusions of metallic phase. Layer 3 is an intermediate zone between layer 2 and the bulk of the metal phase and contains many particles that have detached from layer 2 and moved into the bulk of the melt. The number of these particles is higher for AlN/CB4 than for AlN/CB5.

For the porous samples, the ceramic/metal interface retained its original relief (Fig. 4c) and the interface reaction product enters the bulk of AlN by accompanying melt penetration into the pores. The interaction

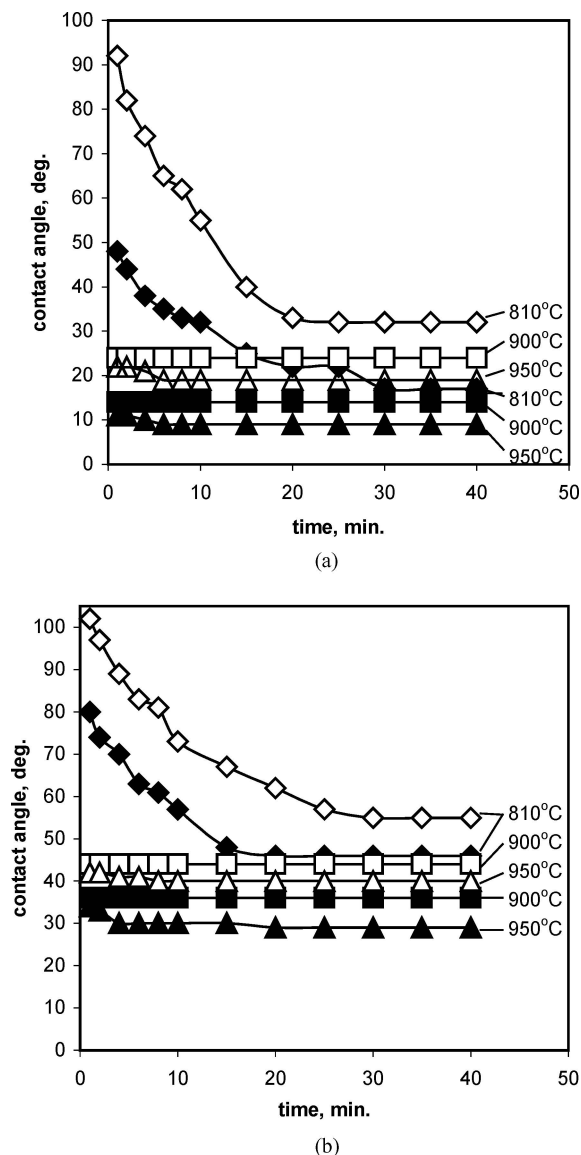


Figure 3 Time and temperature dependencies of contact angles for (a) CB4 and (b) CB5 melts on the pre-oxidized AlN (open points) in comparison with results for fully polished ($R_a = 0.02\text{--}0.03\ \mu\text{m}$) non-preoxidized samples (closed points).

zone comprises randomly distributed sections of different chemical composition (Fig. 4d) with Ti as the main metallic component. The reaction zones for CB5 melt are very similar in distribution of elements.

Microprobe analysis for the dense substrates shows that layer 1 has similar composition for both melts, containing components in atomic ratio $\text{Ti}_{1.0}/\text{N}_{0.7\text{--}0.9}/\text{Cu}_{0.01\text{--}0.04}/\text{Ag}_{0.02\text{--}0.1}/\text{Al}_y$, where $y = 0.02\text{--}0.08$ for CB4 and less than 0.01 for CB5. Layer 2 is similar in composition but contains less N and Al and more Cu and Ag. Typical composition ratio for dark areas of layer 2 is $\text{Ti}_{1.0}/\text{N}_x/\text{Cu}_{0.03\text{--}0.7}/\text{Ag}_{0.1\text{--}0.4}/\text{Al}_y$, where $x = 0.6\text{--}0.8$ with $y_{\text{max}} = 0.02$ for the CB4 melt and $x = 0.4\text{--}0.6$ with $y_{\text{max}} = 0.01$ for the CB5 melt. For both melts, the light areas of layer 2 are silver-copper phases; particles detached from the interface in layer 3 are of the same composition as the dark areas in layer 2; the compositions of bulk melt in layer 3 and near the top of the drop show Cu-based Cu-Ag phase without the presence of Ti or N and Ag-based Ag-Cu phase

with a small quantity of N (up to ~ 1 at.%) and no Ti. Inclusions have been observed near the top of the drop with composition $\text{Ti}_{1.0}/\text{N}_{0.1\text{--}0.3}/\text{Cu}_{0.2\text{--}0.5}/\text{Ag}_{0.2\text{--}0.5}$ for the CB4 melt and $\text{Ag}_{1.0}/\text{Cu}_{0.3}/\text{Ti}_{0.2\text{--}0.4}/\text{N}_{0.01}$ for the CB5 melt. Typically 0.1–0.8 at.% Al was detected at all investigated points for both melts, though for CB4 melt a few points, located mainly in the interface layer 1 or near the top of the drop, registered 1–5 at.% Al. Levels of 0.01–0.09 at.% Y were indicated in all layers for the CB4 melt and in layers 1 and 2 for the CB5 melt.

Pre-oxidized samples (Fig. 5) show a zone comprising two continuous layers 1 and 2, which are thicker for the CB4 melt with the higher Ti content, with many inclusions evident in the solidified melt near the reaction zone for the CB4 sample. While no oxide film is detectable on the surface of AlN on Back-Scattered Electron Images (BEIs), one is evident on corresponding oxygen X-ray maps. Microprobe results for the film are similar for both melts. They give compositions of two stoichiometric atomic ratios: (1) $\text{Al}/\text{O} = 1/1.5$ with 0 or 1.4 at.% Ti and (2) $\text{Al}/\text{O} = 1/2.5\text{--}4.6$ with 11 to 32 at.% Ti. The stoichiometric ratio obtained for layer 1 is $\text{Ti}_1/\text{O}_{0.5\text{--}0.6}/\text{Cu}_{0\text{--}0.15}/\text{Ag}_{0\text{--}0.02}$ and for layer 2 $\text{Ti}_1/\text{O}_{0.4\text{--}0.5}/\text{Cu}_{1\text{--}1.2}/\text{Ag}_{0.01\text{--}0.1}$. Inclusions in CB4 alloy near layer 2 are of composition $\text{Ti}_1/\text{Cu}_{0.7\text{--}1.1}/\text{Ag}_{0.6\text{--}0.9}/\text{O}_{0.3\text{--}0.4}$. Similar inclusions in CB5 alloy have composition $\text{Cu}/\text{Ag}_{0.6}/\text{Ti}_{0.4}/\text{O}_{0.2}$. Small quantities of N and Y were detected at some points in the interaction zone and adjacent metallic phase and Al was detected at all analysed positions.

4. Discussion and conclusions

Registered atomic ratios of elements for the dense samples indicate that both reaction product layers 1 and 2 (Fig. 4a and b) are composed of non-stoichiometric titanium nitride TiN_{1-x} with $x = 0.1\text{--}0.6$. The lowest values of x (highest N) were observed immediately adjacent to the ceramic for both melts. The presence of detectable quantities of Ag and Cu in layer 1 can be due to metallic inclusions between TiN grains. In the course of time, for further TiN formation, N must diffuse through the solid layer of reaction product. This barrier hampers the process and as a result lower N content is observed in layer 2. Considerable inclusions of metallic phase between nitride grains in layer 2 give higher Ag and Cu contents for the analyzed points. The results of the present study are in agreement with results of ref. [11] for the similar systems $\text{AlN}/72\text{Ag-}28\text{Cu-}1$ or 5Ti (wt.%) at 1000°C . The results of [11] show the presence of two layers at the interface. That adjacent to the ceramic is $\text{TiN}_{0.7}$. However, the second layer is identified as a compound of the $(\text{TiCuAl})_6\text{N}$ type. The latter was not evident in the present study. However, if its thickness was less than $1\ \mu\text{m}$, it would not have been detected.

The quantities of Al registered in the liquid phase and reaction zone, exceed by about 100 times the permitted content of Al in CB4 and CB5 brazes (0.001% according to the BrazeTec GmbH Technical Datasheet). Clearly, this is Al released from decomposition of AlN during interaction. As there were no points registered

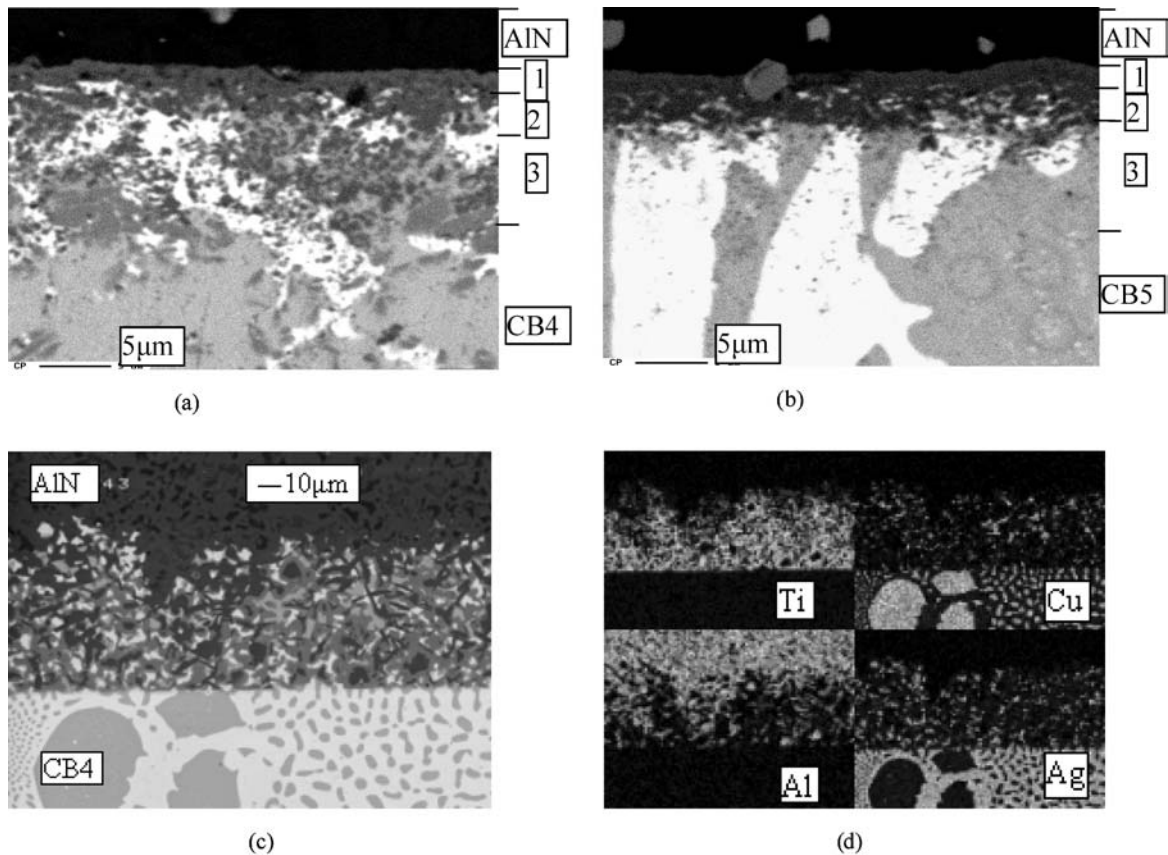


Figure 4 SEM images of the interface microstructure for dense and porous AlN in contact with CB4 and CB5 melts (temperature-time regime: 810°C-40 min, 900°C-40 min, 950°C-40 min): (a) CB4/dense AlN, (b) CB5/dense AlN, (c) CB4/porous AlN with (d) corresponding elemental X-ray maps.

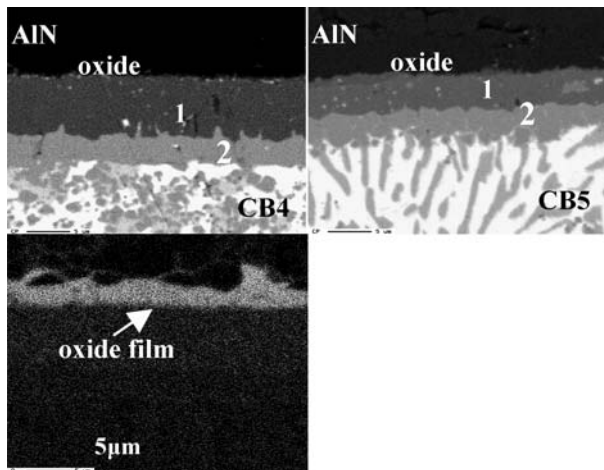


Figure 5 SEM images of the interface microstructure for pre-oxidized AlN in contact with CB4 and CB5 melts (temperature-time regime: 810°C-40 min, 900°C-40 min, 950°C-40 min) with corresponding to CB4 image oxygen X-ray map.

with stoichiometric atomic ratio Al/O as 2/3, it cannot be concluded that there is much or any Al₂O₃ at the interface or in the melt.

Conclusions concerning the interface microstructure for porous samples can be drawn on the basis of comparison of X-ray maps for the porous samples with data for the dense samples. The interface zone for the porous ceramic is composed of randomly distributed TiN_{1-x}, AlN and Cu-Ag alloy.

Registered atomic ratios of elements for pre-oxidized samples indicate that layer 1 (Fig. 5a and b) is composed of non-stoichiometric titanium oxide TiO_{0.5-0.6}. The presence of detectable quantities of Ag and Cu in layer 1 can be due to metallic inclusions between TiO grains. Layer 2's compositions are different from layer 1's and for both melts can be written as Ti₁Cu_{1-1.2}O_{0.4-0.5}, which corresponds to a compound of type Cu₂Ti₂O. It should also be noted that according to element ratios and Fig. 5c, part of the alumina layer remains on the AlN surface and contains inclusions of non-stoichiometric TiO.

The main reaction product observed in the present study for pre-oxidized ceramic (non-stoichiometric TiO) differs significantly from the main product (non-stoichiometric TiN) registered after interaction of non-preoxidized AlN with CB4 and CB5. Moreover, no TiN was registered as an interaction product with the pre-oxidized AlN. Thus, the interface interaction of AlN/CB4,5 couples after pre-oxidation of AlN is replaced in the regime under study by Al₂O₃/CB4,5 interaction. That results in poorer wettability as generally Al₂O₃ is wetted worse than AlN by liquid metals.

The increased contact angles reported herewith for a porous wetted surface can be explained qualitatively by applying an argument used by Dettre and Johnson [12-13]. These authors found for spreading over a porous or heterogeneous surface that the observed advancing contact angle θ will generally be larger than given by equilibrium considerations. They argue that the drop

periphery advances to the equilibrium value of θ via a series of metastable configurations and might not overcome an energy barrier in passing from one such configuration to the next. The vibration energy of the drop and the particularities of the pore geometry encountered will influence the response of the drop periphery to each particular energy barrier. The presence of these energy barriers for the porous surface results in an increase of the effective contact angle as observed in the present work.

The following explanation can be proposed for the absence of significant differences in wettability for the two levels of roughness of AlN. Due to the high chemical affinity of titanium to nitrogen, the melt reacts with and modifies the surface simultaneously with spreading. Macro contact angle depends on the roughness of the new surface relief. The relief for cases under study is not defined by the extent of previous polishing, but by the roughness of the created interface products. Roughness of the new interface was also considered to influence the final contact angle for the systems TiN/Al and AlSi11 [9].

Acknowledgments

The authors are grateful to The Royal Society of UK for visitorships to enable N. Yu. Taranets to carry out this research at the University of Sheffield (Project refs. No AMM/UA/13402/01A and 15458).

References

1. N. FROUMIN, N. FRAGE and M. DARIELL, in Proc. 10th Internat. Ceramic Congress. Part C, edited by P. Vincenzini (Techna, Faenza, 2003) p. 733.
2. A. TSOGA, S. LADAS and P. NIKOLOPOULOS, *Acta Mater.* **45** (1997) 3515.
3. O. DEZELLUS, F. HODAJ, C. RADO, J. N. BARBIER and N. EUSTATHOPOULOS, *ibid.* **50** (2002) 979.
4. J. LOPEZ-CUEVAS, H. JONES and H. V. ATKINSON, *Mater. Sci. Eng. A.* **266** (1999) 161.
5. YU. V. NAIDICH and N. YU. TARANETS, *J. Mater. Sci.* **33** (1988) 3993.
6. J. C. LABBE and G. BRANDY, *Rev. Int. Hautes. Temper. Refract. Fr.* **26** (1990) 131.
7. N. SHINOZAKI KAKU and K. MUKAI, *Trans. JWRI, Special Issue* **30** (2001) 161.
8. YU. V. NAIDICH and V. S. ZHURAVLEV, in *Poverhnostnie yavleniya v rasplavah i obrazuyuschisya iz nih tverdyh fazah* (Kabardino-Balkarskoe Knizhnoe Izdatel'stvo, Nal'chik, 1965) p. 245 (in Russian).
9. N. SOB CZAK, K. PIETRZAK, A. WOJCIECHOWSKI, W. RADZIWILL, M. KSIAZEK and L. STOB IERSKI, *Trans. JWRI* **30** (2001) 173.
10. G. ROSAZZA PRIN, T. BAFFIE, M. JEYMOND and N. EUSTATHOPOULOS, *Mater. Sci. Eng. A* **298** (2001) 34.
11. R. E. LOEHMAN and A. P. TOMSIA, *Acta Metall. Mater.* **40** (1992) S75.
12. E. JOHNSON and R. H. DETTRE, *J. Phys. Chem.* **68** (1964) 1744.
13. R. H. DETTRE and R. E. JOHNSON, in *Wetting*, edited by E. Rideal (Society of Chemical Industry, London, 1967) p. 144.

*Received 31 March
and accepted 18 July 2004*